

Primljen / Received: 27.7.2021.

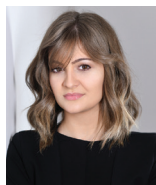
Ispravljen / Corrected: 26.11.2021.

Prihvaćen / Accepted: 29.11.2021.

Dostupno online / Available online: 10.12.2021.

## Comparison of cover meter and ground penetrating radar performance in structural health assessment: case studies

### Authors:



**Ksenija Tešić**, MCE  
University of Zagreb  
Faculty of Civil Engineering  
[ksenija.tesic@grad.unizg.hr](mailto:ksenija.tesic@grad.unizg.hr)



Assist.Prof. **Ana Baričević**, PhD. CE  
University of Zagreb  
Faculty of Civil Engineering  
[ana.baricevic@grad.unizg.hr](mailto:ana.baricevic@grad.unizg.hr)  
Corresponding author



Assist.Prof. **Marijana Serdar**, PhD. CE  
University of Zagreb  
Faculty of Civil Engineering  
[marijana.serdar@grad.unizg.hr](mailto:marijana.serdar@grad.unizg.hr)

Professional paper

**Ksenija Tešić, Ana Baričević, Marijana Serdar**

### Comparison of cover meter and ground penetrating radar performance in structural health assessment: case studies

An essential step in the condition assessment of reinforced concrete structures and evaluation of the residual capacity is the determination of the arrangement and quantity of reinforcement as well as the geometry of the structural elements. The objective of this paper is to present the fundamentals in the application of two non-destructive methods, cover meter and ground penetrating radar, in the determination of the above structural features. A comparison of the two methods is presented and their capabilities, advantages and disadvantages are shown through nine case studies.

#### Key words:

reinforced concrete, reinforcement, concrete cover, non-destructive methods, practical application

Stručni rad

**Ksenija Tešić, Ana Baričević, Marijana Serdar**

### Usporedba učinkovitosti tragača armature i georadara u ocjeni stanja konstrukcija: primjeri iz prakse

Neizostavan korak u ocjenjivanju stanja armiranobetonskih građevina te procjeni preostale nosivosti jest utvrđivanje rasporeda i količine armature i geometrije konstrukcijskih elemenata. Cilj rada je prikazati osnovna načela u korištenju dviju nerazornih metoda, to jest pomoću tragača armature i georadara, tijekom određivanja navedenih karakteristika konstrukcije. Kroz devet primjera iz prakse prikazana je usporedba dviju metoda te su istaknute njihove mogućnosti, prednosti i nedostatci.

#### Ključne riječi:

armirani beton, armatura, zaštitni sloj betona, nerazorne metode, primjena u praksi

## 1. Introduction

Each structure, depending on its use, must be designed and built to meet the basic requirements for structures and other requirements during its service life, i.e., conditions specified in the Building Act and separate regulations [1]. Experience shows that many concrete structures show a significant degree of deterioration after only twenty to thirty years of use due to the interaction of mechanical actions and environmental influences [2]. According to the Technical Regulation for Engineering Structures [3], the owner is responsible for the maintenance of the structure. Maintenance includes an annual basic inspection, a main inspection every ten years for buildings and every five years for bridges, towers and other engineering structures, as well as additional inspections governed by separate regulations for each type of structure. If these inspections, and thus proper maintenance, are not carried out systematically and proactively, the structures suffer from premature and uncontrolled deterioration, which has a negative impact on their safety and usability, as the earthquakes in Croatia in 2020 clearly demonstrated.

The limited knowledge about the behaviour of damaged concrete structures and the lack of systematic and reliable methods for their estimation, maintenance, and repair contribute to an increase in the total life cycle costs of structures and lead to reduced usability, functionality, and safety [4]. Accurate determination of the causes of degradation requires comprehensive knowledge of material and structural properties, degradation mechanisms, and methods for detecting these mechanisms [5] and is a critical step for successful repair of structures [6].

The first step in properly evaluating the condition of a structure is to select an appropriate testing method. Many devices that may be of interest in this regard are currently available on the market. Their applicability depends on numerous factors, such as the type of structure, the degree of deterioration, the exposure class, and also the data needed to assess mechanical resistance and structural stability. This information can be obtained initially through visual inspection, but also through destructive and non-destructive testing. The use of non-destructive testing (NDT) is limited to certain cases in our practise, although its application offers a number of advantages. For example, advances in the development of NDT methods have enabled the visualisation of

results and the use of augmented reality [7], which in turn allows engineers to view the interior of elements in real time and in space. As for the application of NDT methods, protocols and criteria for evaluating the behaviour of materials and structures based on the corresponding results would still need to be developed.

In the condition assessment of reinforced concrete structures, the basic step in performing investigation work is to locate the reinforcement and determine the thickness of the concrete cover. This is especially important for structures for which there is no project documentation and whose reconstruction is the first step in evaluating the existing condition. The devices used today for this purpose, the so-called cover meters, usually work on the principle of eddy currents. The price, speed of testing and simplicity of analysis of the results make this method very popular among civil engineers. However, like any other NDT method, it has some limitations that affect the reliability of the results. This is especially true for structures with a considerable thickness of concrete cover, either in the form of final treatment by plaster or simply in the form of concrete cover. The aim of this paper is to show the possibility of using ground penetrating radar (GPR) for the same purpose, in order to allow a more accurate reconstruction of the project documentation. Therefore, the paper focuses on the basic operating principles of both devices, with emphasis on the areas of application, advantages and shortcomings, which are explained with some practical examples.

## 2. Test methods and practical examples

### 2.1. Test methods

The amount and distribution of reinforcement, the thickness of concrete cover, and the reconstruction of the geometry of the structural elements presented in this article were determined using the Profometer 650 AI cover meter from Proceq and the StructureScan Mini XT ground penetrating radar ( $f = 2.7$  GHz) from GSSI and Proceq GP 8000 ( $f = 0.2 - 4$  GHz) (Figure 1). The measurement range of the cover meter is up to 8 cm, while the maximum signal penetration depth of the StructureScan Mini XT and Proceq GP 8000 ground radars is 60 cm and 80 cm, respectively. The analysis of the results collected with the GPR was performed using the GSSI Radan 7 software.



Figure 1. Testing devices: a) Profometer 650 AI, b) GPR StructureScan Mini XT, c) GPR GP 8000

### 2.1.1. Operating principle of cover meter

A cover meter is a device used to locate reinforcement in concrete. The principle of operation of a cover meter is shown in the following figure (Figure 2). Alternating current is induced in the coil, which generates an alternating magnetic field. The presence of reinforcing steel in the alternating magnetic field leads to the occurrence of eddy currents, which also form a magnetic field. This leads to a change in coil impedance, which serves as a basis for determining the thickness of the concrete cover and the diameter of the reinforcement [8].

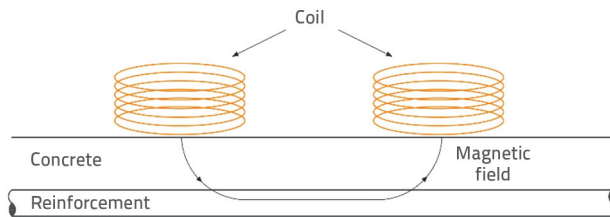


Figure 2. Operating principle of cover meter

Inspection is performed by dragging the device along the line, which detects only the bars that are perpendicular to the drag line. Therefore, in most cases, inspection involves multiple line checks in two directions forming a network. Measurement accuracy is limited when reinforcement intersects with installed grids, anchors and other metals, when aggregates with magnetic properties are present in the concrete and when the concrete cover is thicker.

### 2.1.2. Operating principle of GPR

The operation of the GPR is based on the emission of electromagnetic waves into the material so that the position of objects located below the surface can be determined. In most cases, the GPR consists of a transmitting antenna (transmitter) that emits electromagnetic waves that are reflected back when they hit an object. The reflected wave is registered by the receiving antenna (receiver) (Figure 3a). The recording of the registered wave is called an A-scan (Figure 3b). The travel time of the wave is recorded on one axis, and the energy of the reflected wave is recorded on the other axis.

In GPR testing, scanning is performed along a defined line. During this scanning, waves are continuously transmitted into the material, and the reflected waves are registered by the receiving antenna. The two-dimensional reconstruction of the waves reflected along



Figure 3. a) GPR system, b) A-scan

the depth following a defined line results in a radargram or B-scan. The horizontal axis indicates the GPR position in the area of interest, while the vertical axis indicates the two-way travel time (TWT) or depth (Figure 4). The radiated energy is approximately cone-shaped [9], so the waves are reflected before the device is directly over the object. The waves then have a slightly longer travel time to the receiver, so cylindrical objects, such as rebar, form a typical hyperbolic shape on the radargram when scanned perpendicular to their direction. The radargram is usually displayed in black and white, and the intensity is defined by the amplitude of the reflected wave. In the most common radargram types, the highest positive value of the amplitude corresponds to the areas displayed in white colour, while the highest negative value corresponds to the areas displayed in black colour.

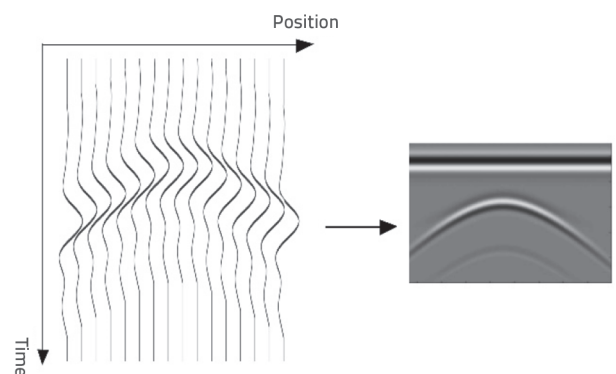


Figure 4. Establishment of a radargram (right side) through association of A-scans

An object is any obstacle whose dielectric properties differ from those of the surrounding material. The amount of reflected energy can be estimated by calculating the reflection coefficient  $R$ , as shown in the following expression [10]:

$$R = \frac{\sqrt{\epsilon_{r2}} - \sqrt{\epsilon_{r1}}}{\sqrt{\epsilon_{r1}} + \sqrt{\epsilon_{r2}}} \quad (1)$$

where  $\epsilon_{r1}$  and  $\epsilon_{r2}$  are the relative dielectric constants of the surrounding material and the material of the object. This means that part of the energy is reflected, while the remaining energy penetrates into deeper layers. The relative dielectric constants for materials of interest for estimating the state of structures

are listed in the following table (Table 1). The polarity of the amplitude and the strength of the reflection depend on the ratio of the dielectric constants: The greater the difference between these values, the greater the strength of the reflection. Concrete and dry sand have similar dielectric constants and therefore the reflection between these two materials would be weak. On the other hand, a pipe filled with water in concrete would produce

a strong positive reflection because the dielectric constant of water is high compared to the constant of concrete. In addition, the contact of concrete with air produces a highly visible negative reflection. In the case of a metal, the dielectric constant is not numerically defined, but it is assumed that this material reflects all electromagnetic energy. Metallic objects, such as rebars, can be recognised by their strong hyperbolic reflections with a positive sign.

**Table 1. Relative dielectric constants of materials [11, 12]**

Material	Relative dielectric constant $\epsilon_r$ [-]
Air	1
Pure water	81
Dry concrete	4-10
Moist concrete	10-20
Wood	2-6
Dry sand	2-6
Dry clay	2-6
Dry soil	4-10
Moist soil	10-30

Some of the signal energy is dissipated during propagation of electromagnetic waves through the material. The attenuation of the signal depends on the nature of the material through which the wave moves. If the material is moist and there are salts in the pores, the conductivity increases and the signal loss is greater than in a dry material without salt. Under such conditions, the efficiency of GPR tests is questionable because much of the energy is lost as the signal passes through the material.

In addition to the described efficiency of signal penetration, which depends on the nature of the material through which the signal propagates, the efficiency also depends on the central frequency of the GPR antenna. These two phenomena are interrelated, so that the possibility of signal penetration decreases with an increase in frequency and vice versa. However, the resolution of the reflection of the investigated area improves with an increase in frequency. Frequency-dependent resolution has two components, vertical and horizontal [13]. Vertical resolution defines the ability to detect two closely spaced objects as two separate occurrences at depth, while horizontal resolution defines the detection of two objects at the same depth in the GPR test direction. Although radar frequencies from 500 MHz to 2.5 GHz are used for condition assessment of reinforced concrete structures [14], the characteristics of the device differ significantly in this range. Roughly speaking, the size of an object must be at least 10 % of the wavelength to be detected by GPR, while the distance between two adjacent objects in the GPR test direction must be at least one wavelength for them to be detected as two separate events [15]. This means that GPR with the central signal frequency of 500 MHz would not detect rebars less than 20 mm in diameter in concrete, nor two separate objects if they are less than 20 cm apart. On the other

hand, GPR with a frequency of 2.5 GHz would not detect the rebars with a diameter of less than 4 mm that are less than 4 cm apart.

The presence of moisture reduces the wave propagation velocity. The velocity of wave propagation can be estimated as follows [16]:

$$v = \frac{c_{air}}{\sqrt{\epsilon_r}} \quad (2)$$

where  $c_{air}$  is the velocity of wave propagation through air (300 mm/ns). If the wave propagation velocity and the wave travel time from the transmitter to the object and then back to the receiver ( $t$ ) are known, the depth of an object ( $d$ ) can be estimated according to Equation (3).

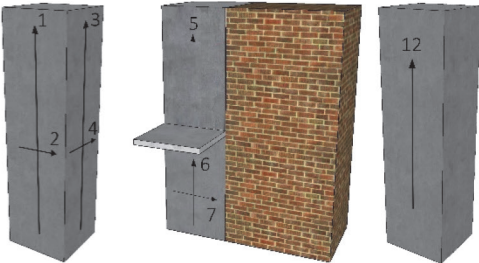
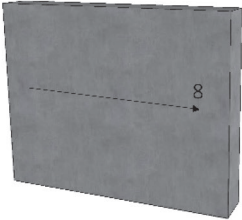
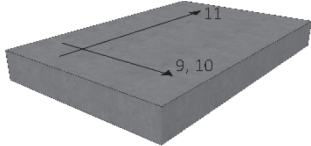
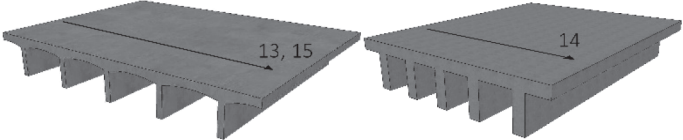
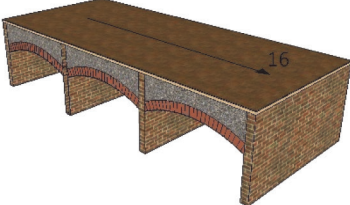
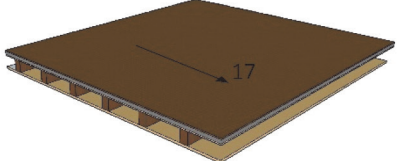
$$d = v \cdot \frac{t}{2} \quad (3)$$

The wave propagation time is measured by GPR, which means that the accuracy of object depth estimation depends on the estimated velocity of wave propagation. The wave propagation velocity can be estimated according to Equation (2) and based on the dielectric constants (Table 1). This is the least accurate method of determining the velocity. Another option is to calculate the velocity according to equation (3) when the depth of the object is known. Another way to estimate the wave propagation velocity is to base this estimate on the hyperbolic reflections in the radargram.

## 2.2. Case studies

A total of nine case studies are presented, tested on a total of five structures. They range from the simplest example of locating reinforcement in reinforced concrete columns to reconstructing a floor structure using a completely non-destructive method. As part of the project to reconstruct buildings after the earthquake that struck Croatia in March and December 2020 [17-19], two structures were tested to determine the type and amount of reinforcement and to estimate the structural capacity. Since the project documentation was available for these structures, it was necessary to confirm the data from the project documentation by verification, i.e., to determine if there were any discrepancies. For the second two structures, the project documentation was not available and the structural capacity had to be determined because the purpose and use of these structures had to be changed. The last structure was tested as part of the renovation of a historic building. All examples presented in this paper were selected on the territory of the Republic of Croatia in 2021. Testing positions were selected with great care considering that uncertainties in the interpretation of results may frequently occur when testing is conducted by non-destructive methods. The measuring points on structural elements were selected in such a way to enable access to elements from several sides. This is important in cases when additional testing of an element is needed due to ambiguity of results.

Table 2. Overview and designation of radargrams

Tested element	Radargram positions and designations	Antenna frequency
Column		2.7 GHz
Wall		2.7 GHz
Monolithic reinforced concrete slab		2.7 GHz
Ribbed floor structure		2.7 GHz
Massive vaulted floor structure		0.2 – 4 GHz
Wooden floor structure		0.2 – 4 GHz

Radargram designations and directions, as well as antenna frequencies corresponding to GPRs by which the radargram was obtained, are presented in Table 2. Examples used in this paper involve non-destructive testing of columns, wall, monolithic reinforced concrete slab, ribbed floor structures, massive vault structure, and wooden floor structure.

### 3. Test results

#### 3.1. Localisation of reinforcement by non-destructive methods

Figure 5 shows the procedure for determining the location of reinforcement in the column using radargrams. Radargrams 1 and 3 were used to determine the location of the stirrups in the column, while the longitudinal reinforcement was determined using radargrams 2 and 4. The peaks of the hyperbola clearly define the position of the rebars, while the distance between the peaks represents the spacing between each rebar. The test was also performed with a cover meter and the results obtained were in complete agreement with the GPR results.

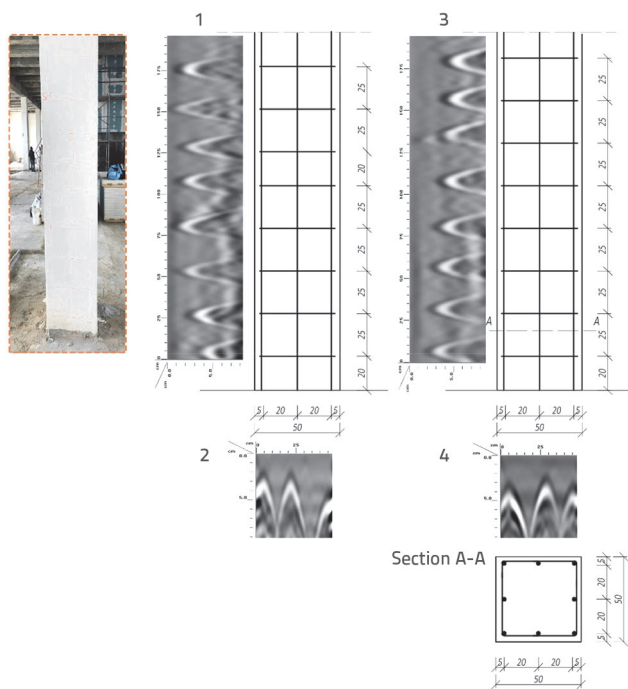


Figure 5. Determination of column reinforcement arrangement (all four sides)

The column presented represents the case where a simple analysis is sufficient to determine the proper arrangement of reinforcement. However, this is not always the case for columns in typical reinforced concrete structures. A greater thickness of plaster can be a limiting factor in locating reinforcement with the cover meter. Such examples are often found in older buildings where the plaster may be as thick as 5 cm. Such an example is shown in Figure 6. The average distance between the reinforcement and the surface was about 7 cm (3.5 cm for the

plaster and 3.5 cm for the concrete cover), so the reinforcement could not be detected with the cover meter and localization was only possible with GPR.

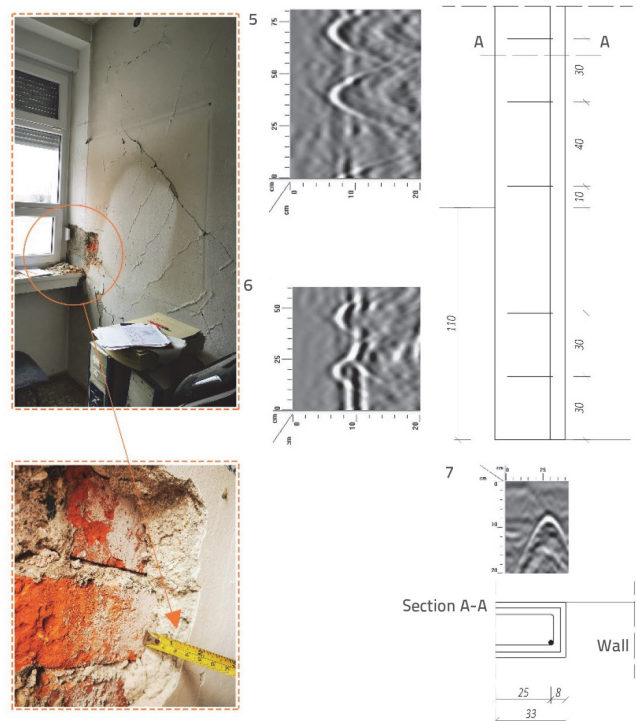


Figure 6. Determination of column reinforcement arrangement from one side only

The determination of reinforcement overlap, which is a challenge for both devices, is shown in the following example. The cover meter cannot visualise this phenomenon, that is, it could suspect its presence based on the estimate of the reinforcement diameter, as in our case. In the case of the wall shown in Figure 7, the diameter of 40 mm was determined by the cover meter.

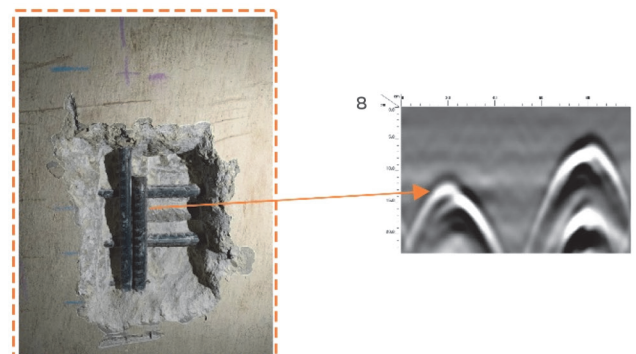


Figure 7. Opening concrete cover to confirm bar overlap

On the other hand, the GPR resolution is usually not sufficient to detect overlaps as two separate bars. In some cases, however, they can be detected as double-shifted hyperbolas, as was the case with the tested wall (Figure 7). This phenomenon does not



This example shows an obvious advantage of using GPR instead of a cover meter. This advantage stems from the principle of operation of the GPR, which allows scanning and visual inspection of the "discovered" area. An interpretation based solely on the use of the cover meter would likely lead to incorrect conclusions. The first layer of reinforcement, i.e., the only layer detected by the cover meter, would likely be defined as longitudinal reinforcement, thus underestimating the effective depth of the slab.

However, there are also cases where the GPR method is not appropriate for locating reinforcement. Figure 10, left, shows the radargram obtained when testing a column of a reinforced concrete structure on which no hyperbolic reflections (indications of the presence of reinforcement) are visible. After opening the column at this exact location, it was found that there was a wire lath under the cover, Figure 10, centre, which was part of the final treatment of this column. The wire lath was observed at a distance of 1.5 cm from the surface of the column. It is assumed that the tightly laid wires completely reflected the electromagnetic waves, preventing the energy from reaching the reinforcement of this column. In this narrow space, the signal is "trapped" between the surface and the wire lath, so that several successive reflections from this surface can be realized in a short time. The reflected waves can be registered by the receiving antenna and are seen on the radargram in the form of approximately equal reflections at approximately equal intervals along the depth. This phenomenon is called "ringing" [20].

In this case, the distribution of the reinforcement was determined with the cover meter. Due to the large diameter of the reinforcement of this column, it was possible to determine the distribution of the reinforcement without having to open the concrete cover, although the wire lath was present.

### 3.2. Determining cover thickness by non-destructive methods

In this section, the results of the cover meter are compared with those of the GPR.

In the case of the cover meter, it was not necessary to specify initial parameters, while in the case of the GPR, the results depend mainly on the dielectric constant. In all four cases shown in Table 3, the dielectric constant was determined based on the known depth of the structure. First, the inspection was performed using the GPR and cover meter, then the structure was opened and the actual thickness of the concrete cover was measured. The dielectric constants were then determined using equations (2) and (3). The estimated values of the dielectric constants are: column -  $\epsilon_r = 6.7$ , wall -  $\epsilon_r = 6.5$ , and slab -  $\epsilon_r = 7.5$ . The dielectric constant determined in this way represents the value that applies locally and to the tested part of the structure. Taking into account the types of structures and the exposure of each part of the structure to environmental influences, constant values of the dielectric constant were assumed for the whole structure.

The first case in which the results were compared concerns a reinforced concrete column (Example 1). This comparison shows a very good agreement between the results obtained with the two instruments. The difference in the average cover thickness is only 2.5 mm. These results are quite expected since the cover thicknesses are within the safe measurement range of both instruments (15 - 48 mm), the spacing between rebars is 20-25 cm for stirrups and 20 cm for longitudinal reinforcement, and there are no other metal structures in the vicinity. These conditions are ideal for both devices, so that the test results can be clearly interpreted.

The specifications of the cover meter state that the measurement range of the concrete cover thickness is up to 8 cm. For this reason, a wall was tested (Example 2) where all cover thicknesses at the measurement point (between 64 and 86 mm) were initially known. Deviations in the cover meter measurements can already be observed at cover thicknesses of 64 to 69 mm, with deviations sometimes reaching 20 mm. At the same time, the GPR shows stable results without deviations from the actual cover thicknesses.

The last example was analysed for the case of a monolithic reinforced concrete slab presented in the previous section (Examples 3 and 4). As mentioned before, the cover meter detected a reinforcement layer, which is assumed to be an overlay. The difference between the measurements of the two devices is more obvious compared to the previous case. The thickness of the concrete cover measured by the cover meter is greater than the data provided by the GPR. It is suspected that in this case the second layer of reinforcement (longitudinal reinforcement) influenced the results of the cover meter and that some of the values displayed are larger than those of the actual concrete cover because the cover meter provides thicknesses that are between the cover thicknesses of the overlay reinforcement and the longitudinal reinforcement. This resulted in a larger standard deviation ( $\pm 20.8$  mm). On the other hand, the GPR provides data that is fairly consistent. This can also be observed for the longitudinal reinforcement of the slab, where the average thickness of the concrete cover is very large, 156.5 mm (Example 4). Considering that the reinforcement is at great depth and the signal is not as clear as for shallower reinforcement layers, the concrete cover thicknesses are consistent.

### 3.3. Additional possibilities of Ground Penetrating Radar (GPR)

An unavoidable advantage of the GPRs is that this device allows estimation of the geometry of the studied structure based on radargrams. This section describes an approach to the analysis of radargrams obtained during the testing of floor structures. The aim of the tests is to estimate the geometry of the structural elements and to determine the positions of these elements. In addition, it is possible to determine the presence and dimensions of other structural elements, such as floor layers, and to locate voids and other similar defects. The analysis is based on the



Table 3. Comparison of cover meter and GPR results in the determination of concrete cover

	Cover meter	GPR
<b>MODEL 1</b> Column		
	<b>Results with 99% reliability (mm)</b>	
	$26.4 \pm 3.9$	$28.9 \pm 3.9$
<b>MODEL 2</b> Wall		
	<b>Results with 99% reliability (mm)</b>	
	$83.4 \pm 6$	$78.5 \pm 5.7$
<b>MODEL 3</b> Monolithic reinforced concrete slab (overlay reinforcement)		
	<b>Results with 99% reliability (mm)</b>	
	$59 \pm 11.7$	$44.3 \pm 1.8$
<b>MODEL 4</b> Monolithic reinforced concrete slab (longitudinal reinforcement)	Not applicable (concrete cover thickness exceeds range of the measuring device)	
	<b>Results with 99% reliability (mm)</b>	
	-	$156.5 \pm 3$

observation of the shapes of the reflections and the polarities of the amplitude of the reflected waves.

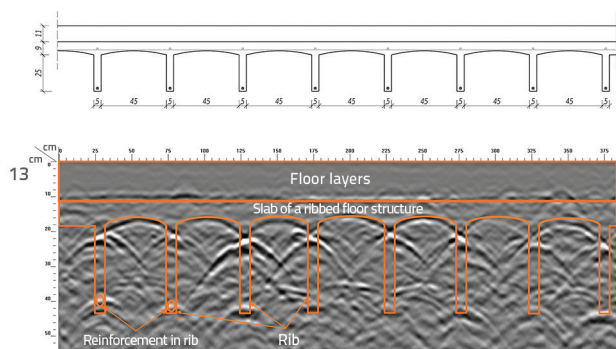


Figure 11. GPR reconstruction of ribbed floor structure based on radargram 13

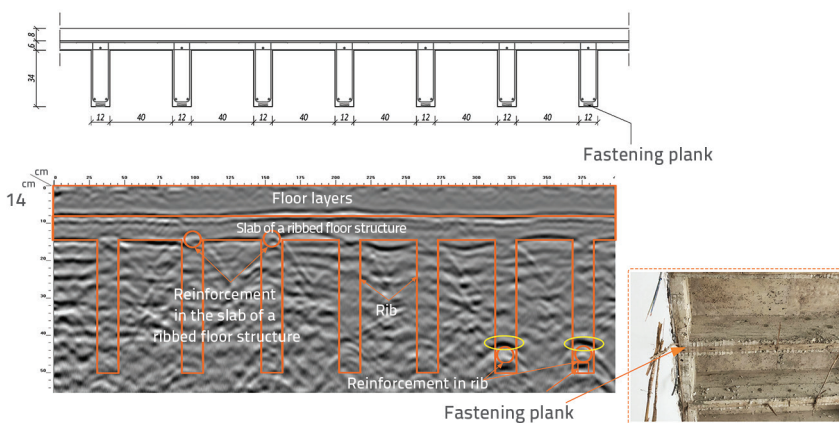


Figure 12. GPR reconstruction of ribbed floor structure based on radargram 14.

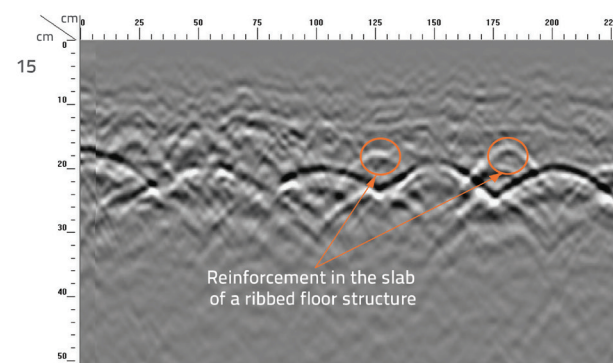


Figure 13. Determination of the presence of reinforcement in the slab of the ribbed floor structure

Four types of floor structures are presented: ribbed floor structure with concrete arch vault, ribbed floor structure, massive floor structure and wooden floor structure.

The first linear reflection on the radargrams of the floor structure mainly corresponds to the end of the floor layers and the beginning of the concrete slab. For such element types, where several different material types are present, one should be very careful

when analysing the dimensions along the depth. A more accurate analysis of depth requires the selection of specific dielectric constants for each material if there is a significant difference between them. A typical feature of ribbed floor structures is repeatable negative reflections (concrete-air) corresponding to the bottom edges of the slab, where the axial spacing is equal to the spacing between the ribs. The following figures show examples of ribbed structures with curved (Figure 11) and flat (Figure 12) bottom edges of the slab.

When testing this type of elements, the presence and position of some structures/objects cannot be clearly determined due to a large number of dense reflections. For example, in the previous case with the vaulted edge of the slab, it was difficult to determine the position of the reinforcement in the slab because the waves were reflected from the bottom edge of the slab. In such cases, as mentioned before, the same type of radargram is made at several measurement positions so that more reliable conclusions can be drawn.

One of them can be seen in Figure 13, where hyperbolic marks over the positions corresponding to the rib positions confirm the presence of reinforcement in the slab. Similarly, the presence of distribution steel in the slab was confirmed by testing in the direction parallel to the spread of the ribs from the top of the floor structure. However, the spacing of this distribution steel differed from that indicated in the project documentation. In this case, the extended testing required testing of the slab from below as well as testing of the ribs. Based on the results of these

extended tests, conclusions were finally drawn about the location and arrangement of the reinforcement.

Negative reflections of irregular shape occurring on radargrams may indicate the presence of voids, irregularities, segregation, etc. One such occurrence is highlighted in yellow in Figure 12, where black reflections can be seen above the reinforcement in the rib. In this case, they are believed to indicate significant segregation where the fastening plank is connected to the rest of the structure. Be that as it may, the depth of the objects studied here is about 45 cm, and in such cases the analysis of the results becomes quite difficult. At such depths, significant signal loss occurs, and the appearance of noise can overlay the reflections of the objects. In these cases, additional processing of the signals can partially improve the quality of the analysis.

In the following case, the second-floor ceiling is a massive vaulted floor structure, with the vaults located between the walls of the basement. The ceiling of the second floor is a wooden floor structure with wooden beams in one direction. Using the radargram made perpendicular to the direction of propagation of the vaults, the span of the vaults and their height and thickness were estimated, as shown in Figure 14. It is assumed that the thicknesses of the floor layers correspond to the floors of masonry buildings constructed at

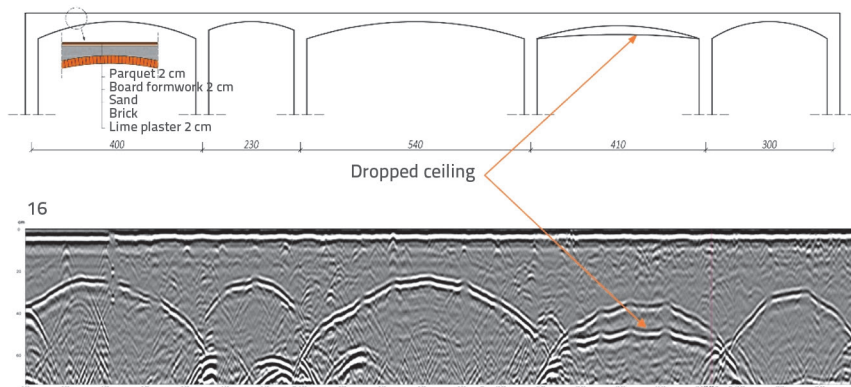


Figure 14. GPR-based estimation of span, height of vaults, and presence of dropped ceiling

the time of the construction of the studied building, as indicated in [21]. This radargram shows negative reflections corresponding to waves reflected from the bottom edge of the vault. It is assumed that the dielectric constants of sand and bricks are similar and that, according to equation (1), most of the energy is transferred during the transition from one material to the other. For this reason, no reflection can be observed at this point in radargram, but only the lower reflection, which corresponds to the joint reflection between brick, plaster and air.

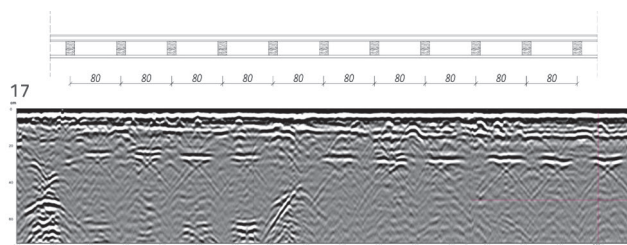


Figure 15. Determining distance between wooden joists.

In addition to estimating the span and height of vaults, it is also possible to determine the presence of dropped ceilings and estimate their height. The first reflection at the lower edge of the vault (brick, plaster - air) has a negative sign. However, the next reflection at the top edge of the dropped ceiling (air - dropped ceiling) has a positive sign. It is assumed that the resolution is not sufficient to detect the thickness of the dropped ceiling, so only the first reflected amplitude (air - dropped ceiling) is registered. When testing wooden floors, a large number of waves reflected in the upper zone (floor layers, top edge of the slab) does not allow clear identification of the beam geometry. For this reason, the distances of beams from wooden floors were determined using an indirect method based on the interaxial distance of reflections from the bottom edge. It should be noted that when testing wood structures whose dielectric constant of the material is close to the constant of air ( $\epsilon_r \approx -2$ ), the test can be improved by wetting the wood to increase the difference in dielectric constants of the materials and thus the strength of the reflection between wood and air.

## 4. Discussion

Based on the results presented in this paper, appropriate conclusions were drawn regarding the advantages and disadvantages of the studied non-destructive methods (Table 4).

Both devices are most suitable for locating longitudinal reinforcement in slabs and for identifying stirrups in beams/columns. Because the maximum penetration depth of the GPR is several times greater than that of the cover meter, the GPR (unlike the cover meter) can locate reinforcement with concrete cover greater than 8 cm. Another

difference between the two methods is that the GPR can determine the location of multiple reinforcement layers in the cross-section. The cover meter, on the other hand, recognizes two closely spaced layers as a single layer and is not able to distinguish signals, which often proves to be a problem with thin-walled reinforced concrete elements ( $d < 15$  cm). However, the presence of a dense reinforcement mesh in the surface layer, such as a wire lath, can completely prevent further penetration of GPR electromagnetic waves into the cross-section. In such a case, the metal objects near the surface provide a barrier to the passage of the electromagnetic energy and the reinforcement becomes invisible to the GPR. If the reinforcement must be located in the area of the bearings and joints, where the reinforcement is densest, the results must be interpreted with great caution.

The thickness of the concrete cover has a great influence on the accuracy of the measurement results and is related to the minimum diameter of the reinforcement. The measurement accuracy decreases significantly with increasing concrete cover, but also with the presence of other magnetic materials near the tested zone [22]. The reinforcement diameter can be estimated with the cover meter for cover thicknesses of  $< 4$  cm with an error probability of less than 10 % [22]. For today's modern structures, where the cover thickness corresponds to EC2, the error probability increases considerably and even reaches 100 % for  $c > 7$  cm.

GPR devices that can estimate the diameter of reinforcing bars are not yet available on the market. However, research is being conducted to develop different algorithms to estimate the diameter. For example, the diameter of the first layer of rebar can be estimated approximately from the difference between the depth of the rebar in two directions measured by the GPR device. This is a very simple and fast procedure, but it provides only approximate information, and only for the first layer of reinforcement. On the other hand, advanced radargram analyses allow a more accurate determination of the diameter. The algorithms presented in the current literature are mainly based on the determination of the hyperbolic reflection parameters, on the basis of which the reinforcement diameter can be determined [23-25]. In general, the accuracy of the diameter determination is very sensitive to the presence of noise and other factors affecting the clarity of

Table 4. Application of cover meter and ground-coupled GPR ( $f > 2\text{GHz}$ )

Requested information	Description of the situation	Cover meter	GPR
Localisation of reinforcement	Localisation of the first layer of reinforcement with concrete cover of $< 8\text{ cm}$	Possible	Possible
	Localisation of the first layer of reinforcement with concrete cover of $> 8\text{ cm}$	Not possible	Possible
	Localisation of the second layer of reinforcement	Not possible	Possible
	Localisation of reinforcement in the presence of wire lath	Possible	Not possible
	Estimation of diameter	Possible	Possible, but results are unreliable or require more advanced analysis
	Reinforcement overlap	Possible, but results are unreliable or require more advanced analysis	Possible, but results are unreliable or require more advanced analysis
Determination of concrete cover thickness	Concrete cover of first layer of reinforcement up to $6\text{ cm}$	Possible	Possible
	Concrete cover of first layer of reinforcement from $6\text{ to }8\text{ cm}$	Possible, but results are unreliable or require more advanced analysis	Possible
	Concrete cover of first layer of reinforcement above $8\text{ cm}$	Not possible	Possible
	Cover thickness for the first layer of reinforcement in structures with two layers of reinforcement	Possible, but results are unreliable or require more advanced analysis	Possible
	Cover thickness for the second layer of reinforcement	Not possible	Possible
Other	Geometry of structural elements	Not possible	Possible
	Probability of corrosion	Not possible	Possible, but results are unreliable or require more advanced analysis
	Voids, delamination, pipes, prestressing cables, etc.	Not possible	Possible

Legend:  
■ Possible  
■ Possible, but results are unreliable or require more advanced analysis  
■ Not possible

the hyperbolas [23]. Moreover, each of these algorithms requires advanced analysis of the signals, which is the main reason why they have not been used in practice so far. Reinforcement overlap cannot be reliably determined by any of the considered methods, since they rely on the analysis of indirect events that are not originally measured by the devices.

For structures with a single reinforcement layer, with concrete cover thicknesses up to  $6\text{ cm}$ , and with reinforcement spacing greater than  $10\text{ cm}$ , both cover meter and GPR are convenient for determining concrete cover thickness. If the concrete cover thickness varies between  $60\text{ and }80\text{ mm}$ , the measuring accuracy of the cover meter decreases and beyond this value, the measurement with this device becomes impossible. In structures with two layers of reinforcement, the GPR can be used to determine the concrete cover for both layers of reinforcement, while the cover meter can only do this for the first layer and with considerable inaccuracy. It is important to note that the accuracies analysed in this study are only applicable in determining the concrete cover if the dielectric constant has been properly determined. In this work, the dielectric constant was determined locally and assumed to be constant for the entire structure. However, if individual parts of the structure are exposed to different environmental conditions, this method would not be sufficiently accurate. Indeed, it is quite possible that some parts are subjected to greater chloride or moisture exposure, which would change the dielectric properties of the material and thus the constant. If this is the case, the dielectric

constants must be determined in situ and calibration performed separately for each part of the structure.

This paper does not cover all the possibilities of ground penetrating radar. In addition to locating reinforcement and determining concrete cover thickness, these devices can also be used to obtain information on the geometry of structural elements [26], the corrosion of reinforcement [27], and the location of voids, delamination, prestressing cables, and pipes [28]. The geometry of structural elements is determined by observing the shape of the reflection of objects and their polarity. Again, the dielectric constant plays an important role in determining the exact location of detected objects. This analysis can be of great importance in floor structures. Taking into account the thickness of the plaster and the thickness of the structural elements, the depth of the investigated objects is very often at the upper limit of the signal penetration depth (about  $60\text{ cm}$ ). Due to the loss of energy during the penetration of materials, the energy returned after reflection from very deep objects is small in most cases. The amplitude loss can be recovered by subsequent amplification of the signals, but this is usually accompanied by the appearance of noise, which makes interpretation of the results much more difficult. In any case, one should be very careful with results that do not provide a clear determination of the position and shape of objects. It is recommended that such discrepancies be resolved by testing with other methods or by opening the structure. The evaluation of corrosion is based mainly on the observation of the change in amplitude of waves reflected from corroded bars [29] and on

the change in the wave frequency spectrum [30]. The causes of corrosion, i.e., moisture and chlorides, and the consequences of corrosion, i.e., rust and cracks, lead to attenuation of signals, so the analysis of corrosion aims to find the area where significant loss of electromagnetic energy has occurred. In order to draw a plausible conclusion that attenuation has occurred, information on the amplitude of a sound concrete and uncorroded bars is essential [31], or attenuation should be demonstrated by the change in the signal through successive measurements over a period of time [32]. In this type of analysis, special attention must be paid to the use of signal processing to preserve the originality of the reflected waves, since their strength is the starting point of the analysis. Ground penetrating radar can also be used to locate major damage, which can be seen in the form of larger cracks, delamination, and weakening of the cross section.

## 5. Conclusion

The paper presents the advantages and disadvantages of cover meter and ground penetrating radar (GPR) devices in determining the location of reinforcement and the thickness of concrete cover. The two devices are compared using nine case studies. The use of GPR for non-destructive reconstruction of the geometry of floor structures is also presented. The use of these two methods is of exceptional importance in estimating the condition of existing structures in cases where project documentation is not available.

It has been noted that in some cases, such as a thick concrete slab with two layers of reinforcement, there may be difficulties in making measurements with cover meter. The difficulties

manifest themselves mainly in the impossibility of detecting reinforcement and in the determination of an unreliable value that lies between the cover thicknesses of two reinforcement layers. Such misinterpretations can lead to an underestimation of the bearing capacity. In such cases, ground penetrating radar has proven to be the more appropriate and reliable tool.

Moreover, as shown in this paper, the GPR has some additional advantages. For example, it can not only locate reinforcement, but also simultaneously detect the presence of objects and other changes in the cross-section of reinforced concrete elements. During the same test, it is possible to determine the geometry of the elements, the presence of prestressing cables and pipes, segregation, fragmentation, voids, etc. GPR can also be used to perform tests without removing the concrete cover even if asphalt, plaster or other surface layers are present. However, these applications require a somewhat more advanced analysis of the signals as well as knowledge of the basic principles of electromagnetic theory. The analysis becomes even more complex when dealing with complicated geometries with many details that often cause reflection of the waves. In such cases, it is recommended to confirm possible uncertainties by additional tests with destructive or non-destructive methods.

## Acknowledgements

This research is a part of the scientific project Autonomous system for inspection and prediction of integrity of transport infrastructure (ASAP) financed by the European Union from the European Regional Development Fund within the call Investment in Science and Innovation – first call KK.O1.1.1.04.

## REFERENCES

- [1] Hrvatski sabor, Zakon o gradnji, NN 153/2013, Narodne novine, Zagreb, Hrvatska, 2017.
- [2] Mehta, B.Y.P.K., Burrows, R.W.: Building Durable Structures in the 21<sup>st</sup> Century, Concrete International, 23 (2001), pp. 57-63.
- [3] Ministarstvo graditeljstva i prostornoga uređenja, Tehnički propis za građevinske konstrukcije, NN 17/2017, Zagreb, Hrvatska, 2017.
- [4] Cusson, D.: Durability of repaired concrete structures, Failure, Distress and Repair of Concrete Structures, ed. N. Delatte, Woodhead Publishing Limited and CRC Press LLC, New Delhi, India, pp. 296-321, 2009.
- [5] Lounis, Z.: Aging highway bridges, Canadian Consulting Engineer, 48 (2007) 1, pp. 30-34.
- [6] Lukovic, M.: Influence of interface and strain hardening cementitious composite (SHCC) properties on the performance of concrete repairs, TU Delft, Delft, Netherlands, 2016.
- [7] Ohtsu, M.: Introduction, Innovative AE and NDT Techniques for On-Site Measurement of Concrete and Masonry Structures, ed. M. Ohtsu, Springer, Dordrecht, Germany, pp. 1-4, 2016.
- [8] Raupach, M., Büttner, T.: Concrete Repair to EN 1504: Diagnosis, Design, Principles and Practice, CRC Press, London, 2014.
- [9] Wang, Z.W., Zhou, M., Slabaugh, G.G., Zhai, J., Fang, T.: Automatic detection of bridge deck condition from ground penetrating radar images, IEEE Transactions on Automation Science and Engineering, 8 (2011) 3, pp. 633-640, <https://doi.org/10.1109/TASE.2010.2092428>.
- [10] Clem, D.J., Schumacher, T., Deshon, J.P.: A consistent approach for processing and interpretation of data from concrete bridge members collected with a hand-held GPR device, Construction and Building Materials, 86 (2015), pp. 140-148. <https://doi.org/10.1016/j.conbuildmat.2015.03.105>.
- [11] Daniels, D.J.: Ground Penetrating Radar 2<sup>nd</sup> Edition, The Institution of Electrical Engineers, London, 2008.
- [12] Torgovnikov, G.I.: Dielectric Properties of Wood and Wood-Based Materials, Springer-Verlag, New York, 1993.
- [13] Annan, A.P.: Electromagnetic Principles of Ground Penetrating Radar, Ground Penetrating Radar: Theory and Applications, ed. M.H. Jol, : Elsevier B.V, Amsterdam, The Netherlands, pp. 1-40, 2009.
- [14] Tosti, F., Ferrante, C.: Using Ground Penetrating Radar Methods to Investigate Reinforced Concrete Structures, Surveys in Geophysics, 41 (2020) 3, pp. 485-530, <https://doi.org/10.1007/s10712-019-09565-5>.

- [15] Utsi, E.C.: Ground penetrating radar: Theory and practice, Elsevier Ltd., Oxford, United Kingdom, 2017.
- [16] ACI 228.2R-98 – Nondestructive Test Methods for Evaluation of Concrete Structures, Concrete Repair Manual, American Concrete Institute, Farmington Hills, Michigan, USA, 1999.
- [17] Šavor Novak, M., Uroš, M., Atalić, J., Herak, M., Demšić, M., Baniček, M., Lazarević, D., Bijelić, N., Crnogorac, M., Todorčić, M.: Zagreb earthquake of 22 March 2020 – preliminary report on seismologic aspects and damage to buildings, GRAĐEVINAR, 72 (2020) 10, pp. 843-867, doi: <https://doi.org/10.14256/JCE.2966.2020>
- [18] Uroš, M., Šavor Novak, M., Atalić, J., Sigmund, Z., Baniček, M., Demšić, M., Hak, S.: Post-earthquake damage assessment of buildings – procedure for conducting building inspections, GRAĐEVINAR, 72 (2020) 12, pp. 1089-1115, doi: <https://doi.org/10.14256/JCE.2969.2020>
- [19] Pojatina, J., Barić, D., Anđić, D., Bjegović, D.: Structural renovation of residential building in Zagreb after the 22 March 2020 earthquake, GRAĐEVINAR, 73 (2021) 6, pp. 633-648, doi: <https://doi.org/10.14256/JCE.3195.2021>
- [20] Solla, M., Lorenzo, H., Pérez-Gracia, V.: Ground penetrating radar: Fundamentals, methodologies and applications in structures and infrastructure, Non-Destructive Techniques for the Evaluation of Structures and Infrastructure, eds. B. Riviero, M. Solla, CRC Press Taylor & Francis Group, New York and London, pp. 89–111, 2016.
- [21] Peulić, Đ.: Konstrukcijski elementi zgrada, Croatia knjiga, Zagreb, 2002.
- [22] Drobiec, Ł., Jasiński, R., Mazur, W.: Accuracy of eddy-current and radar methods used in reinforcement detection, Materials (Basel), 12 (2019) 7, <https://doi.org/10.3390/ma12071168>.
- [23] Xiang, Z., Ou, G., Rashidi, A.: Integrated Approach to Simultaneously Determine 3D Location and Size of Rebar in GPR Data, Journal of Performance of Constructed Facilities, 34 (2020) 5, [https://doi.org/10.1061/\(asce\)cf.1943-5509.0001502](https://doi.org/10.1061/(asce)cf.1943-5509.0001502).
- [24] Chang, C.W., Lin, C.H., Lien, H.S.: Measurement radius of reinforcing steel bar in concrete using digital image GPR, Construction and Building Materials, 23 (2009) 2, pp. 1057–1063, <https://doi.org/10.1016/j.conbuildmat.2008.05.018>.
- [25] Mechbal, Z., Khamlichi, A.: Determination of concrete rebars characteristics by enhanced post-processing of GPR scan raw data, NDT and E International, 89 (2017), pp. 30–39, <https://doi.org/10.1016/j.ndteint.2017.03.005>.
- [26] Pérez-Gracia, V., Caselles, O., Clapés, J., Osorio, R., Canas, J.A., Pujades, L.G.: Radar exploration applied to historical buildings: A case study of the Marques de Llió palace, in Barcelona (Spain), Engineering Failure Analysis, 16 (2009) 4, pp. 1039–1050, <https://doi.org/10.1016/j.engfailanal.2008.05.007>.
- [27] Tešić, K., Baričević, A., Serdar, M.: Non-Destructive Corrosion Inspection of Reinforced Concrete Using Ground Penetrating Radar: A Review, Materials (Basel), 14 (2021) 4, <https://doi.org/10.3390/ma14040975>.
- [28] Dinh, K., Gucunski, N.: Factors affecting the detectability of concrete delamination in GPR images, Construction and Building Materials, 274 (2021), <https://doi.org/10.1016/j.conbuildmat.2020.121837>.
- [29] Wong, P.T.W., Lai, W.W.L., Sham, J.F.C., Poon, C.S.: Hybrid non-destructive evaluation methods for characterizing chloride-induced corrosion in concrete, NDT and E International, 107 (2019) January, <https://doi.org/10.1016/j.ndteint.2019.05.008>.
- [30] Lai, W.L., Kind, T., Stoppel, M., Wiggerhauser, H.: Measurement of Accelerated Steel Corrosion in Concrete Using Ground-Penetrating Radar and a Modified Half-Cell Potential Method, Journal of Infrastructure Systems, 17 (2013) December, pp. 395–408, [https://doi.org/10.1061/\(ASCE\)IS](https://doi.org/10.1061/(ASCE)IS).
- [31] Diamanti, N., Annan, A.P., Redman, J.D.: Concrete Bridge Deck Deterioration Assessment Using Ground Penetrating Radar (GPR), Journal of Environmental and Engineering Geophysics, 22 (2017) 2, pp. 121–132, <https://doi.org/10.2113/JEEG22.2.121>.
- [32] Dinh, K., Zayed, T., Romero, F., Tarussov, A.: Method for analyzing time-series GPR data of concrete bridge decks, Journal of Bridge Engineering, 20 (2015) 6, pp. 1–8, [https://doi.org/10.1061/\(ASCE\)BE.1943-5592.000067](https://doi.org/10.1061/(ASCE)BE.1943-5592.000067)